IEEE Access
Multidisciplinary | Rapid Review | Open Access Journal

Received December 13, 2019, accepted January 16, 2020, date of publication January 21, 2020, date of current version January 31, 2020.

Digital Object Identifier 10.1109/ACCESS.2020.2968518

A Compact Dual-Wideband Bandpass Filter Based on Open-/Short-Circuited Stubs

GEN-ZHU LIANG AND FU-CHANG CHEN, (Member, IEEE)
School of Electronic and Information Engineering, South China University of Technology, Guangzhou 510641, China

Corresponding author: Fu-Chang Chen (chenfuchang@scut.edu.cn)

This work was supported in part by the Guangdong Natural Science Funds for Distinguished Young Scholars under Grant 2019B151502032, and in part by the Fundamental Research Funds for the Central Universities under Grant 2018ZD07.

ABSTRACT A dual-wideband bandpass filter is proposed and analyzed, which is based on loaded open-/short-circuited stubs. The dual-band filter consists of a second-order bandpass filter and a third-order bandpass filter, which can be designed separately. The bandwidth of two passbands can be adjusted by tuning the impedance and the length of the stubs. A dual-band bandpass filter prototype operating at 2.4/5.2 GHz is designed for demonstration. It shows a low insertion loss of 0.3 dB and wide bandwidth of 51.9% at 2.4 GHz and 23.3% at 5.2 GHz. The filter structure is simple without narrow coupling gap between resonators, which is easy for fabrication.

INDEX TERMS Dual-band bandpass filters, microstrip, stub, wideband.

I. INTRODUCTION

As an indispensable part of the communication systems, microwave filter shoulders the important mission of frequency selection and has been widely used in military and civil fields. In recent years, with the rapid development of modern wireless communication system, frequency spectrum resource is becoming more and more crowded, and single-band bandpass filters can not satisfy the demands of precise spectrum division, so multi-band bandpass filters are increasingly becoming a hot spot of scientific researches and explorations.

To cope with the development of new era and new situation, various approaches of designing dual-band bandpass filter have been proposed [1]–[3]. The most direct way to design a dual-band bandpass filter is combining two single-band filters with different passbands [4], while it suffers from large size. Cascading a bandpass filter and a bandstop filter is another effective method to get dual-band performance [5]. To reduce the circuit size, the spurious frequencies of the stepped-impedance resonators (SIRs) are often used to create the second passband [6]–[9]. A balanced dual-band bandpass filter composed of a direct dual-band bandpass branch with resistively terminated bandstop filter branches connected to the input and output ports is proposed in [10]. A dual-band bandpass filter using transversal filtering structure to obtain wide stopband suppression is presented in [11]. A method to design a selectivity-enhanced SIR dual-band bandpass filter with two open-circuited stubs added at one node of the port coupled-line stages is illustrated in [12]. However, the filters in [10]–[12] fail to reduce the in-band insertion loss, which degrades the filter performance. Ring loaded resonator (RLR) is also a structure commonly used in filter design. In [13], a dual-band differential bandpass filter is designed by coupling two identical stepped impedance square RLRs and its frequency selectivity is improved by utilizing a source-loaded coupling structure. Weng *et al*. [14] used a stepped impedance RLR to design a dual-band bandpass filter with a narrow first passband and a wide second passband and tapped rectangular stub loaded resonators on the input and output ports to obtain a wide stopband. To achieve two wide passbands, dual-band bandpass filers based on the cascade of dual-passband transversal filtering sections with two loading stubs are presented in [15], while the two passbands are frequency-symmetrical, which is difficult to control the center frequency independently. By loading stubs on a two-end short-circuited SIR, the authors in [16] achieved a dual-band filter with wide bandwidth. In [17], a dual-wideband bandpass filter based on short-circuited SIRs is proposed. Wang *et al*. [18] used bridged-T coils to replace transmission line sections to design reduced-size dual-band bandpass filters with wide bandwidths. Slotline structure is also an

The associate editor coordinating the review of this manuscript and approving it for publication was Feng Lin.

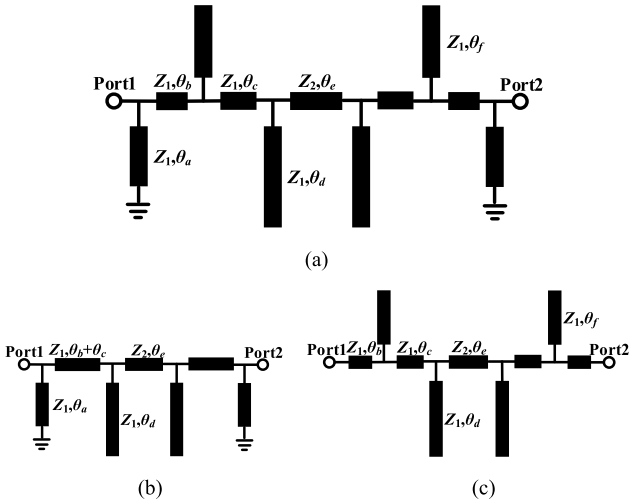

FIGURE 1. Ideal transmission line model of proposed filter. (a) Dual-band bandpass filter. (b) Second-order bandpass filter. (c) Third-order bandpass filter.

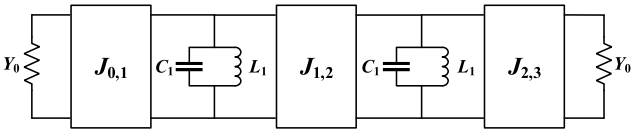

FIGURE 2. Equivalent circuit of the second-order bandpass filter.

effective way to implement a dual-band filter. A dual-band differential filter based on coupled strip-loaded slotline resonators and strip-loaded coupled slotlines is proposed in [19].

Most dual-band filters reported in the literature have a narrow bandwidth, while some dual-wideband filters suffer from complicated structure. In this paper, a simple method to design a dual-wideband bandpass filter is proposed. Fig. 1 shows the ideal transmission line model of the proposed filter, which has the virtues of compact size and simple structure. As no coupling structure is employed, low insertion loss in each passband can be attained. The simulated results show that the 3-dB bandwidths of the filter are 1.74-2.96 GHz at 2.4 GHz and 4.63-5.85 GHz at 5.2 GHz, which is confirmed powerfully by the measured results.

II. ANALYSIS OF THE PROPOSED FILTER

As shown in Fig. 1(a), the proposed dual-wideband filter is comprised of a transmission line loaded with a pair of short-circuited stubs (Z_1, θ_a) and two pairs of open-circuited stubs (Z_1, θ_d, Z_1, θ_f). The characteristic impedances of all stubs are the same (Z_1). When the electrical lengths of the stubs are properly selected, the proposed filter can be considered as a combination of two single-band bandpass filters, which is illustrated in Fig. 1(b) and (c). The analysis of the single-band bandpass filter with a pair of short-circuited stubs and a pair of open-circuited stubs will be given in Part A, then the other single-band bandpass filter with two pairs of open-circuited stubs will be analyzed in Part B. Finally, a dual-band filter can be obtained by combining two single-band bandpass filters, which will be illustrated in Part C.

A. SECOND-ORDER BANDPASS FILTER

The single-band bandpass filter shown in Fig. 1(b) consists of two short-circuited stubs of electrical length θ_a and two open-circuited stubs of electrical length θ_d at the center frequency of the passband. The characteristic impedance of the stubs and transmission line is denoted by Z_1 and Z_2. When the total electrical length of the open-circuited stub, the short-circuited stub and the connecting line between them is a quarter wavelength ($\theta_a + \theta_b + \theta_c + \theta_d = 90°$ in Fig. 1(b)), the combined transmission line can be equivalent to a parallel resonant circuit. In addition, when the electrical length of the connecting line between the open-circuited stubs is a quarter wavelength ($\theta_e = 90°$ in Fig. 1(b)), the connecting line can be regarded as an admittance inverter. So the equivalent circuit of the structure in Fig. 1(b) is a second-order bandpass filter, which is illustrated in Fig. 2.

According to [20], the relationship between the lumped elements values, the admittance inverters values and the characteristic impedance of the stubs and connecting line can be described as

$$C_1 = \frac{\pi}{4\omega_0 Z_1}, \quad L_1 = \frac{1}{\omega_0^2 C_1} \tag{1}$$

$$J_{0,1} = \sqrt{\frac{\pi FBW}{4g_0 g_1 Z_0 Z_1}} \tag{2}$$

$$J_{1,2} = \frac{\pi FBW}{4Z_1\sqrt{g_0 g_1}} = \frac{1}{Z_2} \tag{3}$$

$$J_{2,3} = \sqrt{\frac{\pi FBW}{4g_2 g_3 Z_0 Z_1}} \tag{4}$$

where g_n (n = 0, 1, 2, 3) is the element value of the second-order lowpass filter prototype and Z_0 is the terminal impedance. The center angular frequency and the fractional bandwidth of the bandpass filter is denoted by ω_0 and FBW. The admittance inverters are equivalent to the coupling element between resonators, and the values of them can be deduced on the basis of equations (2), (3) and (4).

As shown in Fig. 1(b), a tapped-line coupling structure is used to feed the quarter wavelength resonator. The coupling strength is determined by the location of the feeding point. Circuit simulation is carried out by AWR Microwave Office. Fig. 3 shows the simulated S-parameter of the second-order bandpass filter centered at 2.4 GHz under different impedances and electrical lengths. The electrical length of the open-circuited stubs and the characteristic impedance of the stubs are fixed at $\theta_d = 56.3°$ and $Z_1 = 80\ \Omega$, respectively. It can be seen that the bandwidth of the bandpass filter can be tuned by adjusting the impedance of the transmission line and the feed position of the quarter wavelength resonator, while a transmission zero in the upper stopband produced by the open-circuited stubs (Z_1, θ_d) is observed.

B. THIRD-ORDER BANDPASS FILTER

As shown in Fig. 1(c), the other single-band bandpass filter consists of a transmission line and four open-circuited stubs.

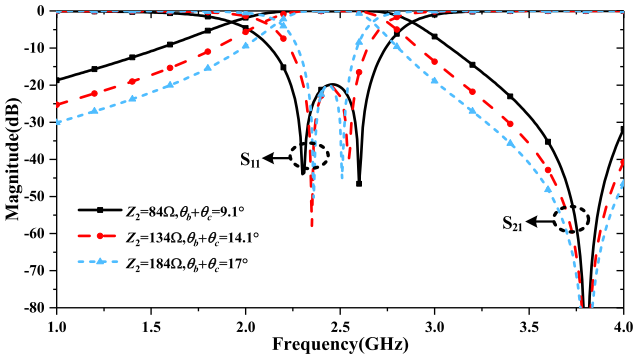

FIGURE 3. Simulated S-parameter of the second-order bandpass filter under different impedances and electrical lengths.

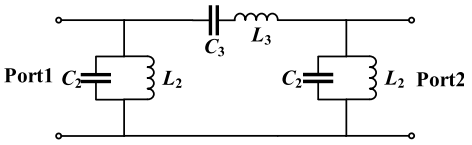

FIGURE 4. Equivalent circuit of the third-order bandpass filter.

The electrical lengths of the longer open-circuited stubs and the shorter ones are denoted by θ_d and θ_f. According to [21], when the total electrical length of the open-circuited stubs and the connecting line θ_c between them is equal to a half-wavelength ($\theta_c + \theta_d + \theta_f = 180°$), this combined line can be equivalent to a parallel resonant circuit. When the electrical length of the connecting line between two longer open-circuited stubs is a half-wavelength, i.e. $\theta_e = 180°$, it can act as a series resonant circuit. The equivalent circuit of structure in Fig. 1(c) is demonstrated in Fig. 4, which is a typical third-order bandpass filter.

On the basis of [22], the relationship between the values of the lumped elements and the impedance of the resonator can be obtained.

$$C_2 = \frac{g_1}{Z_0\omega_0 FBW} = \frac{\pi}{2\omega_0 Z_1}, \quad L_2 = \frac{1}{\omega_0^2 C_2} \tag{5}$$

$$L_3 = \frac{g_2 Z_0}{\omega_0 FBW} = \frac{\pi Z_2}{2\omega_0}, \quad C_3 = \frac{1}{\omega_0^2 L_3} \tag{6}$$

$$Z_1 = \frac{\pi Z_0 FBW}{2g_1} \tag{7}$$

$$Z_2 = \frac{2g_2 Z_0}{\pi FBW} \tag{8}$$

where g_1 and g_2 is the element value of the third-order lowpass filter prototype and Z_0 is the terminal impedance. According to the above equations, the characteristic impedance of the stubs and connecting line can be deduced from the bandwidth of the bandpass filter.

Fig. 5 shows the simulated S-parameter of the third-order bandpass filter centered at 5.2 GHz under different impedances, while maintaining the electrical length of the shorter open-circuited stubs and the connecting line between longer stub and shorter stub ($\theta_f = 27.3°$ and $\theta_c = 0.3°$). It can be found that the bandwidth of the bandpass filter can be controlled by changing the impedances of the stubs

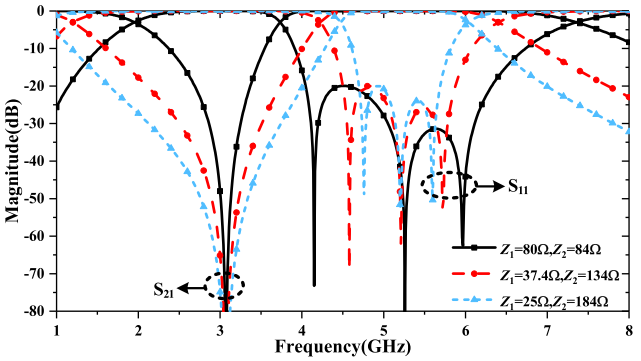

FIGURE 5. Simulated S-parameter of the third-order bandpass filter under different impedances.

and connecting line, while a transmission zero in the lower stopband produced by the longer open-circuited stubs (Z_1, θ_d) is also observed.

C. DUAL-BAND BANDPASS FILTER

A dual-band bandpass filter can be achieved by combining the bandpass filters designed in Part A and Part B. The second-order bandpass filter is used to implement the first passband (f_1), while the third-order bandpass filter is used to realize the second passband (f_2). When f_2 is approximately twice of f_1, two single-band bandpass filters can share the same connecting transmission line (Z_2, θ_e). When $f_2 = Rf_1$, R is the frequency ratio, the electrical length of the connecting line can be selected as the average value of two cases

$$\theta_e = \frac{1}{2}\left(\frac{\pi}{2} + \frac{\pi}{R}\right) \tag{9}$$

To reduce the mutual effect between two single bandpass filters, the electrical lengths of the stubs should be designed properly. To place the transmission zero created by open-circuited stubs (Z_1, θ_d) at the midpoint of the two passbands, the electrical length (θ_d) should be chosen as a quarter wavelength at $(f_1 + f_2)/2$.The electrical length (θ_a) of the short-circuited stub should be selected about a quarter wavelength at f_2, therefore, the input impedance of the short-circuited stub is near an open circuit at f_2, and the loading impact caused by the short-circuited stub on the second passband can be ignored. Similarly, the electrical length (θ_f) of the shorter open-circuited stubs should be as small as possible, resulting in unremarkable effect on the first passband. By choosing the impedances and electrical lengths of the stubs and connecting line reasonably, a dual-band bandpass filter centered at 2.4/5.2GHz can be obtained. The simulation of the lossless transmission line circuit is executed by AWR Microwave Office, and the parameters of the dual-band filter shown in Fig. 1 can be listed as follows: $Z_1 = 80\ \Omega$, $Z_2 = 84\ \Omega$, $\theta_a = 30°$, $\theta_b = 5.2°$, $\theta_c = 5.4°$, $\theta_d = 53.8°$, $\theta_e = 78.4°$, $\theta_f = 29°$ at f_1. The simulated S-parameters of the dual-band filter and the single-band filters are shown in Fig. 6, indicating that each passband of the dual-band filter agrees well with the passband of corresponding single-band filter.

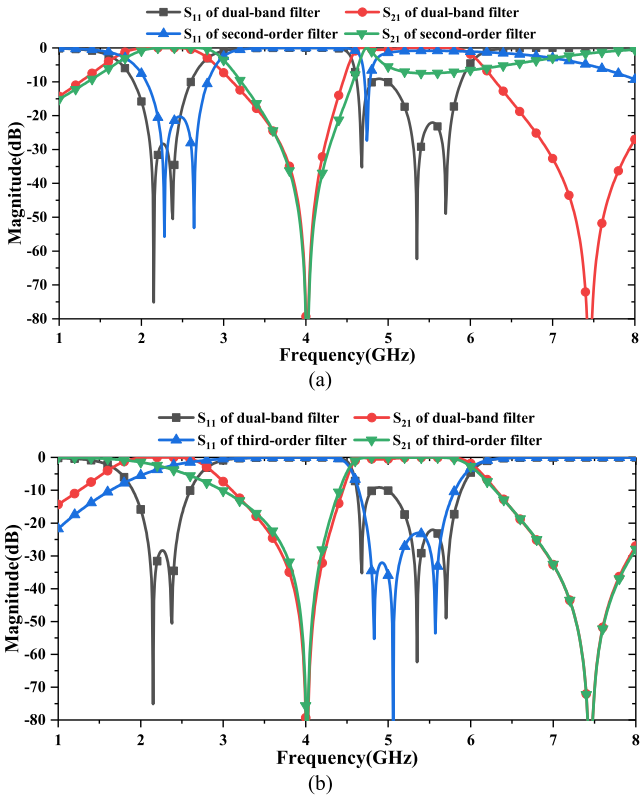

FIGURE 6. Simulated S-parameter of the dual-band filter, second-order filter (a) and third-order filter (b).

III. FABRICATION AND MEASUREMENT

To verify the proposed design method, a dual-wideband bandpass filter centered at 2.4/5.2 GHz is simulated and fabricated. The simulation is carried out on the basis of a substrate with dielectric constant $\varepsilon_r = 2.55$, loss tangent $\delta = 0.0029$ and thickness $h = 0.8$ mm. The configuration of the filter is shown in Fig. 7. The longer open-circuited stubs and connecting line are meandered for miniaturization. The via that connects the microstrip line and the ground plane is denoted by a circle with diameter D. The dimensions of the filter are: $L_1 = 8.1$ mm, $L_2 = 1.1$ mm, $L_3 = 1.8$ mm, $L_4 = 4.2$ mm, $L_5 = 8.5$ mm, $L_6 = 4.9$ mm, $L_7 = 5.7$ mm, $L_8 = 5.1$ mm, $L_9 = 7.1$ mm, $W_1 = 2.3$ mm, $W_2 = 1$ mm, $W_3 = 0.9$ mm and $D = 1$ mm. It owns a total size of 24.4 mm $\times$ 17.5 mm, which is 0.28 λ_g by 0.20 λ_g, where λ_g is the guide wavelength of a 50 Ω microstrip line on the substrate at 2.4 GHz, i.e. the center frequency of the lower passband. The simulation and measurement are carried out by using Zeland IE3D and Agilent 5230A network analyzer.

Fig. 8 shows the simulated and measured responses and a photograph of the fabricated filter. Compared with the simulation results of ideal transmission line model in Fig. 6, in full-wave electromagnetic simulation, the two transmission zeros between two passbands are generated by the longer open-circuited stubs, while the other two transmission zeros on the upper stopband are created by the shorter open-circuited stubs. The measured results indicate that the fractional bandwidth of the filter is 51.9% at 2.4 GHz and 23.3% at 5.2 GHz.

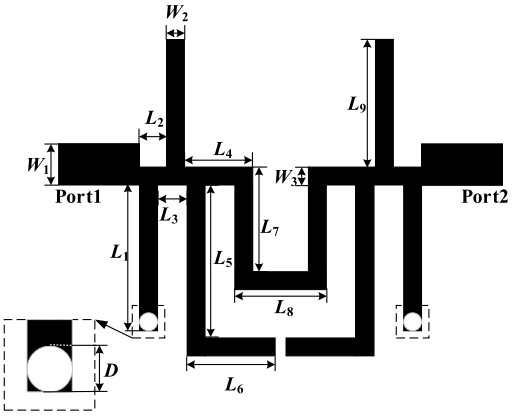

FIGURE 7. Physical layout of the designed dual-wideband bandpass filter.

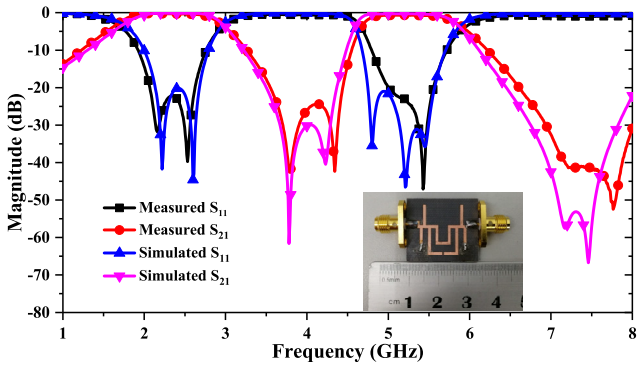

FIGURE 8. Simulated and measured S-parameter of the designed dual-band filter.

TABLE 1. Comparison between this work and other previous DB-BPFs.

References	CFs (GHz)	3-dB FBWs (%)	IL (dB)	RL (dB)	Size ($\lambda_g \times \lambda_g$)
[10]	2.82/3.21	5.2/5.1	1.9/1.7	21.6/16.1	2.76×1.30
[11]	3.78/4.82	11.3/10.7	1.38/1.82	14/33	0.16×0.31
[12]	1.57/2.38	9.9/6.5	1.21/1.95	19/24	--
[13]	2.6/5.8	10.4/3.6	1.1/2.15	>20	0.26×0.34
[14]	2.4/4	8/39	1.4/1	--	0.48×0.09
[17]	2.3/5.25	54/20	0.8/0.8	>20	0.30×0.30
This work	2.4/5.2	51.9/23.3	0.3/0.7	22.1/20.8	0.28×0.20

The return loss is better than 20 dB and the insertion loss is less than 0.3 dB and 0.7 dB in the first passband and second passband, respectively. And the maximum in-band group-delay variations are 4.6 ns and 5.5 ns. The measured results are in good agreement with the simulated results. Table 1 further lists a comparison between this work and other previous dual-band filters, which clearly shows that the proposed filter has wide bandwidths, low insertion loss and compact size.

IV. CONCLUSION

A method for designing a dual-wideband bandpass filter using loaded open-/short-circuited stubs is proposed. The dual-band characteristic is obtained by combining two single-band bandpass filters without increasing the circuit size.

The bandwidth of each passband can be controlled by adjusting the impedance and the electrical lengths of the stubs. The design concept has been validated by fabricating and measuring an experimental filter. The simulated results agree well with the measured results. The designed dual-wideband filter has a compact size and wide bandwidths and operates at 2.4/5.2 GHz, which is suitable for the wireless communication systems, such as WLAN.

REFERENCES

[1] P. Velez, J. Bonache, and F. Martin, "Dual-band balanced bandpass filter with common-mode suppression based on electrically small planar resonators," *IEEE Microw. Wireless Compon. Lett.*, vol. 26, no. 1, pp. 16–18, Jan. 2016.
[2] H. Zhu and A. M. Abbosh, "Single-and dual-band bandpass filters using coupled stepped-impedance resonators with embedded coupled-lines," *IEEE Microw. Wireless Compon. Lett.*, vol. 26, no. 9, pp. 675–677, Sep. 2016.
[3] J. Xu, Z.-Y. Chen, and Q.-H. Cai, "Design of miniaturized dual-band low-pass–bandpass and bandpass filters," *IEEE Trans. Compon., Packag., Manuf. Technol.*, vol. 8, no. 1, pp. 132–139, Jan. 2018.
[4] C.-Y. Chen and C.-Y. Hsu, "A simple and effective method for microstrip dual-band filters design," *IEEE Microw. Wireless Compon. Lett.*, vol. 16, no. 5, pp. 246–248, May 2006.
[5] L.-C. Tsai and C.-W. Hsue, "Dual-band bandpass filters using equal-length coupled-serial-shunted lines and *Z*-transform technique," *IEEE Trans. Microw. Theory Techn.*, vol. 52, no. 4, pp. 1111–1117, Apr. 2004.
[6] J.-T. Kuo and E. Shih, "Microstrip stepped impedance resonator bandpass filter with an extended optimal rejection bandwidth," *IEEE Trans. Microw. Theory Techn.*, vol. 51, no. 5, pp. 1554–1559, May 2003.
[7] S.-F. Chang, Y.-H. Jeng, and J.-L. Chen, "Dual-band step-impedance bandpass filter for multimode wireless LANs," *Electron. Lett.*, vol. 40, no. 1, pp. 38–39, 2004.
[8] Y. Zhang and M. Sun, "Dual-band microstrip bandpass filter using stepped-impedance resonators with new coupling schemes," *IEEE Trans. Microw. Theory Techn.*, vol. 54, no. 10, pp. 3779–3785, Oct. 2006.
[9] M.-H. Weng, H.-W. Wu, and Y.-K. Su, "Compact and low loss dual-band bandpass filter using pseudo-interdigital stepped impedance resonators for WLANs," *IEEE Microw. Wireless Compon. Lett.*, vol. 17, no. 3, pp. 187–189, Mar. 2007.
[10] R. Gomez-Garcia, J.-M. Munoz-Ferreras, W. Feng, and D. Psychogiou, "Balanced symmetrical quasi-reflectionless single-and dual-band bandpass planar filters," *IEEE Microw. Wireless Compon. Lett.*, vol. 28, no. 9, pp. 798–800, Sep. 2018.
[11] L.-T. Wang, Y. Xiong, L. Gong, M. Zhang, H. Li, and X.-J. Zhao, "Design of dual-band bandpass filter with multiple transmission zeros using transversal signal interaction concepts," *IEEE Microw. Wireless Compon. Lett.*, vol. 29, no. 1, pp. 32–34, Jan. 2019.
[12] R. Gomez-Garcia, L. Yang, J.-M. Munoz-Ferreras, and D. Psychogiou, "Selectivity-enhancement technique for stepped-impedance-resonator dual-passband filters," *IEEE Microw. Wireless Compon. Lett.*, vol. 29, no. 7, pp. 453–455, Jul. 2019.
[13] B. Ren, H. Liu, Z. Ma, M. Ohira, P. Wen, X. Wang, and X. Guan, "Compact dual-band differential bandpass filter using quadruple-mode stepped-impedance square ring loaded resonators," *IEEE Access*, vol. 6, pp. 21850–21858, 2018.
[14] M.-H. Weng, S.-W. Lan, S.-J. Chang, and R.-Y. Yang, "Design of dual-band bandpass filter with simultaneous narrow- and wide-bandwidth and a wide stopband," *IEEE Access*, vol. 7, pp. 147694–147703, 2019.
[15] M. A. Sanchez-Soriano and R. Gomez-Garcia, "Sharp-rejection wide-band dual-band bandpass planar filters with broadly-separated passbands," *IEEE Microw. Wireless Compon. Lett.*, vol. 25, no. 2, pp. 97–99, Feb. 2015.
[16] J. Xu, Y.-X. Ji, C. Miao, and W. Wu, "Compact single-/dual-wideband BPF using stubs loaded SIR (SsLSIR)," *IEEE Microw. Wireless Compon. Lett.*, vol. 23, no. 7, pp. 338–340, Jul. 2013.
[17] K.-S. Chin and J.-H. Yeh, "Dual-wideband bandpass filter using short-circuited stepped-impedance resonators," *IEEE Microw. Wireless Compon. Lett.*, vol. 19, no. 3, pp. 155–157, Mar. 2009.
[18] Y.-R. Wang and Y.-S. Lin, "Size-reduction of dual-wideband bandpass filters using bridged-T coils," *IEEE Access*, vol. 7, pp. 42836–42845, 2019.
[19] X. Guo, L. Zhu, and W. Wu, "A dual-wideband differential filter on strip-loaded slotline resonators with enhanced coupling scheme," *IEEE Microw. Wireless Compon. Lett.*, vol. 26, no. 11, pp. 882–884, Nov. 2016.
[20] J.-S. Hong and M. J. Lancaster, *Microstrip Filters for RF/Microwave Applications*. New York, NY, USA: Wiley, 2001.
[21] F.-C. Chen, Q.-X. Chu, J.-M. Qiu, and Z.-H. Chen, "Low insertion loss wideband bandpass filter with six transmission zeros," *Electron. Lett.*, vol. 49, no. 7, pp. 477–479, Mar. 2013.
[22] D. M. Pozar, *Microwave Engineering*, 3rd ed. Hoboken, NJ, USA: Wiley, 2005.